

Supporting information for:

Two novel AIEE-active imidazole/α-cyanostilbene derivatives: photophysical properties, reversible fluorescence switching, and detection of explosives

Yuyang Zhang,^a Jianyan Huang,^a Lin Kong,^{*a} Yupeng Tian,^a Jiaxiang Yang^{*a,b}

Contents:

1. The SEM images of the aggregates.
2. Single crystal data of **M-1**.
3. Photophysical properties of **M-1** and **M-2**.
4. ¹H NMR titration spectra of **M-1** and **M-2**.
5. The detection schematic mechanism for gaseous acid/base.
6. Selective experiments of **M-1** and **M-2** for different derivatives.
7. The Sterne-Volmer plots of compounds **M-1** and **M-2**
8. Time dependent fluorescence quenching efficiency.
9. ¹H NMR titration spectra of **M-1** and **M-2** for PA.
10. Normalized absorption spectrum of PA, 2,4-DNP and the fluorescence spectra of **M-1** and **M-2**
11. Reversibility experiment of fluorescent test strips.

Table S1 Summary of crystallographic data and structure refinement details for **M-1**

Empirical formula	C ₅₆ H ₃₈ N ₄	Temperature (K)	296(2)
Formula weight	766.90	Crystal size (mm)	0.19 × 0.18 × 0.18
Crystal system, Space group	Triclinic, <i>P</i> ī	Absorption coefficient (mm ⁻¹)	0.069
<i>a</i> (Å)	13.463(2)	<i>F</i> (000)	804
<i>b</i> (Å)	13.599(2)	θ range for data collection	1.51-25.00
<i>c</i> (Å)	14.644(2)	Limiting indices	-14 ≤ <i>h</i> ≤ 16, -15 ≤ <i>k</i> ≤ 14, -17 ≤ <i>l</i> ≤ 17
α (°)	73.288(2)	Reflections collected / unique	11738 / 7161 [R(int) = 0.0210]
β (°)	68.720(2)	<i>Data / restraints /</i> <i>parameters</i>	7161 / 0 / 542
γ (°)	60.714(2)	<i>Goodness-of-fit on F</i> ²	2.049
Volume (Å ³)	2158.9(6)	Final R indices [I > 2σ(I)]	<i>R</i> _I = 0.1772 <i>wR</i> ₂ = 0.4773
<i>Z</i>	2	R indices (all data)	<i>R</i> _I = 0.2078, <i>wR</i> ₂ = 0.5093

Table S2 Selected bond distances (Å) and bond angles (°) for compound **M-1**

N(2)-C(23)	1.380(7)	C(23)-N(2)-C(15)	107.6(4)
N(2)-C(15)	1.397(7)	C(23)-N(2)-C(30)	126.8(5)
N(2)-C(30)	1.429(7)	C(15)-N(2)-C(30)	125.3(5)
N(1)-C(15)	1.326(7)	C(15)-N(1)-C(16)	107.2(5)
N(3)-C(37)	1.135(9)	N(1)-C(15)-N(2)	109.1(5)
N(4)-C(51)	1.416(9)	N(1)-C(15)-C(14)	128.4(5)
N(4)-C(44)	1.428(9)	N(2)-C(15)-C(14)	128.4(5)
N(4)-C(45)	1.432(9)	N(2)-C(15)-C(14)	122.4(5)
C(15)-C(14)	1.446(8)	C(13)-C(14)-C(15)	118.3(6)
C(16)-C(23)	1.363(8)	C(23)-C(16)-N(1)	109.6(5)
C(16)-C(17)	1.463(8)	C(23)-C(16)-C(17)	131.4(5)
C(24)-C(23)	1.495(8)	N(1)-C(16)-C(17)	118.9(5)

C(35)-C(36)	1.503(8)	C(16)-C(23)-N(2)	106.4(5)
C(36)-C(38)	1.302(10)	N(2)-C(23)-C(24)	118.6(5)
C(36)-C(37)	1.452(9)	C(38)-C(36)-C(35)	127.1(6)
C(38)-C(39)	1.482(10)	C(37)-C(36)-C(35)	114.0(6)

Table S3 The UV-vis absorbance and fluorescence emission data of compounds **M-1** and **M-2** in different solvents

Compounds	Solvents	λ [a] max	λ [b] max	ϵ ($\times 10^4$) ^[c]	$\Delta\lambda$ [d]	Φ [e]
M-1	toluene	390	494	2.67	5398	0.05
	benzene	390	493	2.67	5357	
	DCM	390	533	2.68	6773	
	THF	389	523	2.93	6589	
	ethyl acetate	387	521	2.98	6649	
	ethanol	388	532	2.87	6976	
	acetonitrile	387	548	2.87	7591	
M-2	DMF	389	548	2.88	7459	0.21
	toluene	400	496	3.39	4838	
	benzene	400	500	3.53	5000	
	DCM	405	534	3.76	5864	
	THF	397	526	3.65	6177	
	ethyl acetate	393	522	3.53	6288	
	ethanol	398	531	3.61	6293	
	acetonitrile	394	547	4.34	7099	
	DMF	396	547	3.39	6970	

[a] Peak position of the longest absorption band. [b] Peak position of fluorescence emission, excited at the absorption maximum. [c] Molar absorptivity (L/cm/mol). [d] Stokes' shift in cm^{-1} . [e] Quantum yields in solid state.

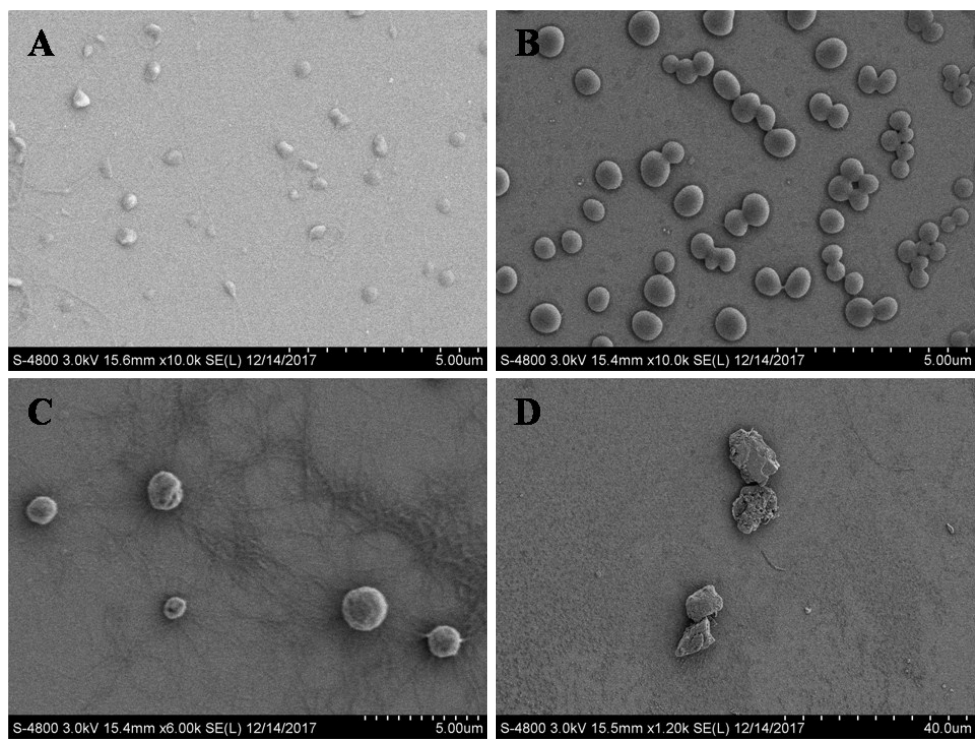


Fig. S1 The SEM images of **M-1** (A, B) and **M-2** (C, D) formed from THF-water mixtures.
(A, C) $f_w = 0\%$; (B, D) $f_w = 90\%$.

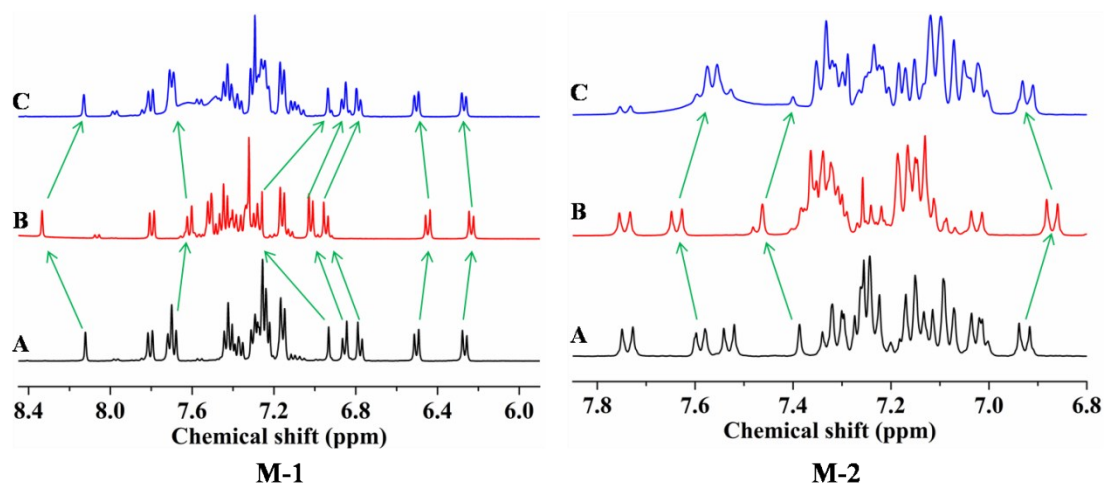


Fig. S2 ^1H NMR spectra of **M-1** and **M-2** in CDCl_3 with **M-1** and **M-2** (A); **M-1** and **M-2** + 2 equivalents TFA (B); **M-1** and **M-2** + 2 equivalents TFA + 5 equivalents TEA (C).

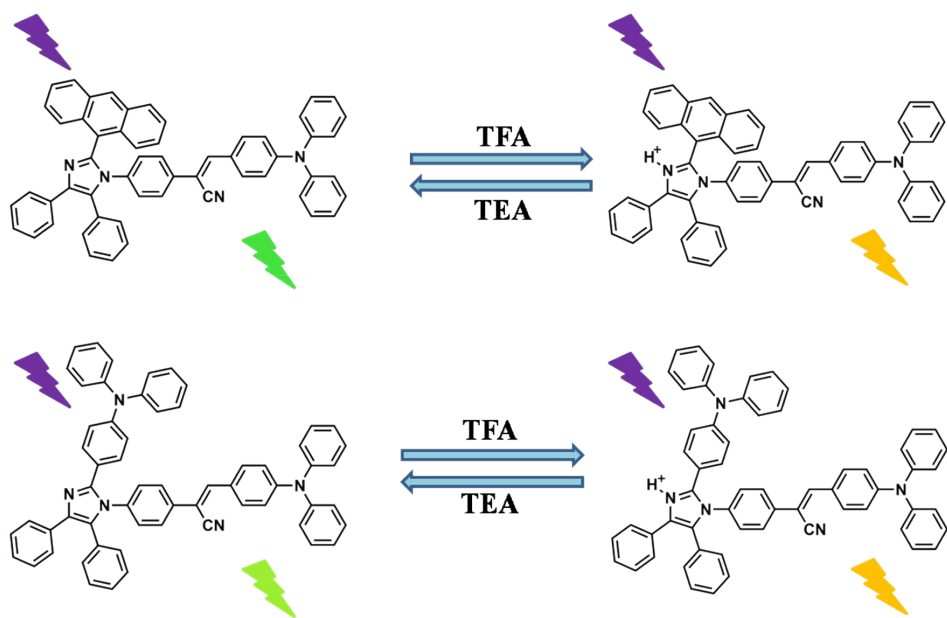


Fig. S3 The detection schematic mechanism for gaseous acid/base with **M-1** and **M-2**.

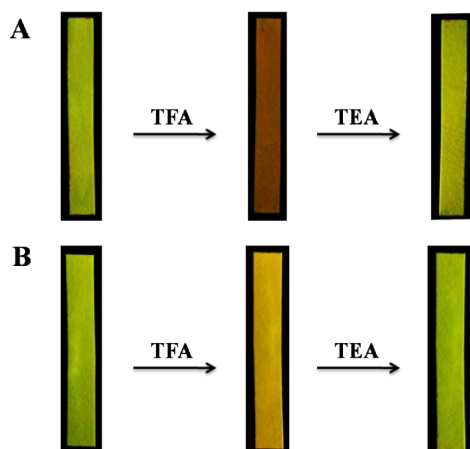


Fig. S4 **M-1** (A) and **M-2** (B) paper samples (left to right: blank, TFA vapor fumed sample, TEA vapor fumed sample after fumed by TFA vapor) recorded under 365 nm UV light (A).

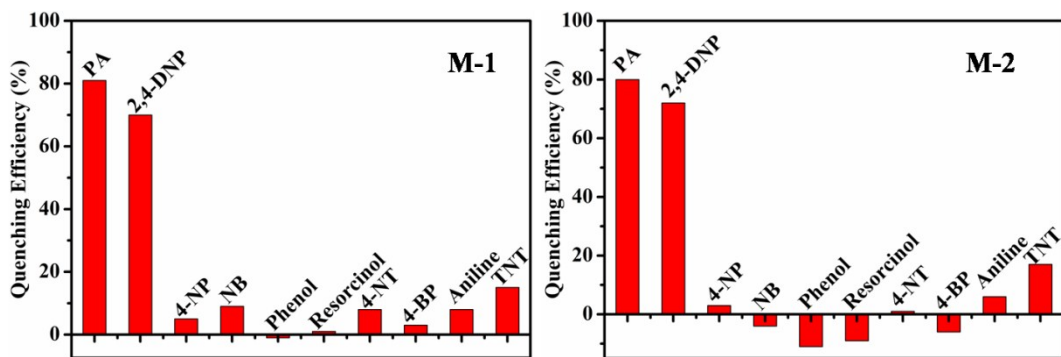


Fig. S5 Degree of fluorescence quenching of compounds **M-1** and **M-2** after addition of 15 equiv of various NACs in THF-water ($f_w = 90\%$) mixture solution.

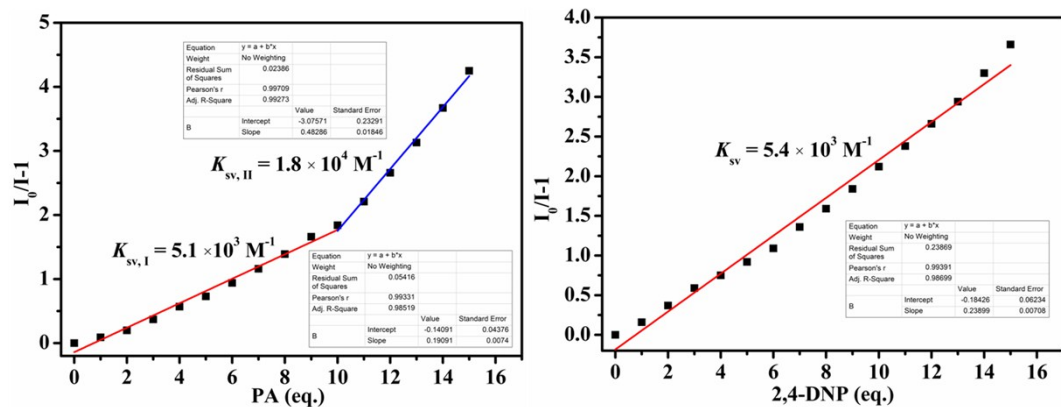


Fig. S6 Plots of ($I_0/I-1$) values of compound **M-1** versus PA and 2,4-DNP concentrations in THF-water ($f_w = 90\%$) mixture solution

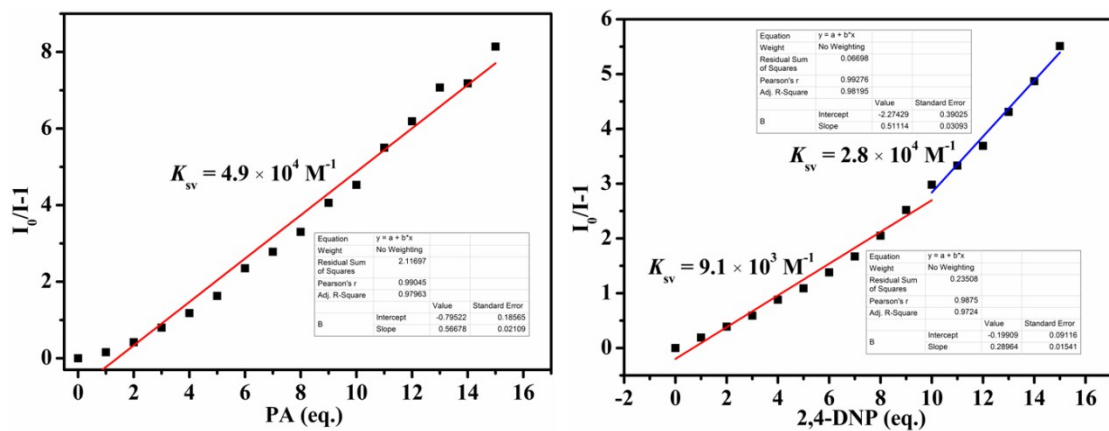


Fig. S7 Plots of (I_0/I_1) values of compound **M-2** versus PA and 2,4-DNP concentrations in THF-water ($f_w = 90\%$) mixture solution

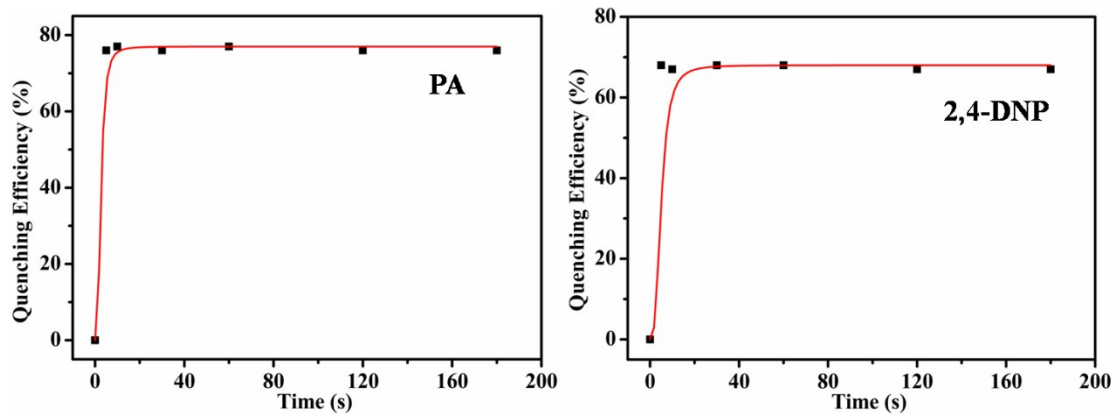


Fig. S8 Time dependent fluorescence quenching efficiency response of **M-1** to PA (15 eq.) and 2,4-DNP (15 eq.)

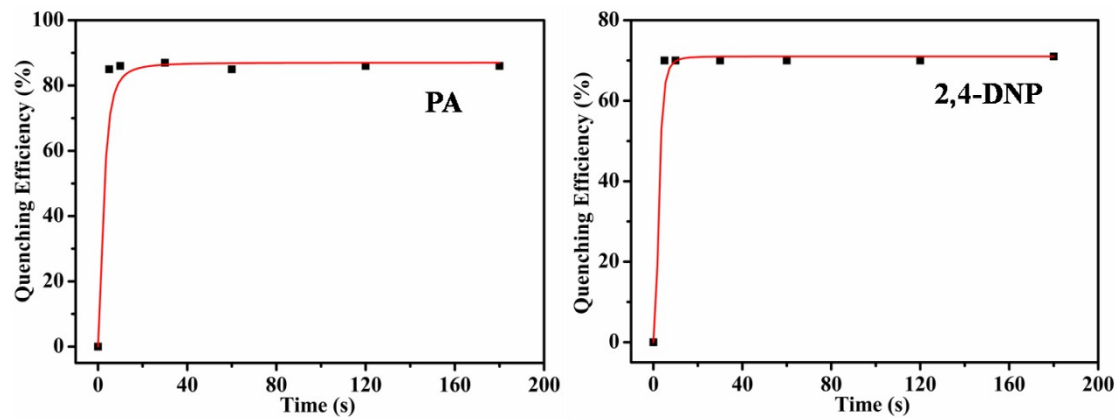


Fig. S9 Time dependent fluorescence quenching efficiency response of **M-2** to PA (15 eq.) and 2,4-DNP (15 eq.)

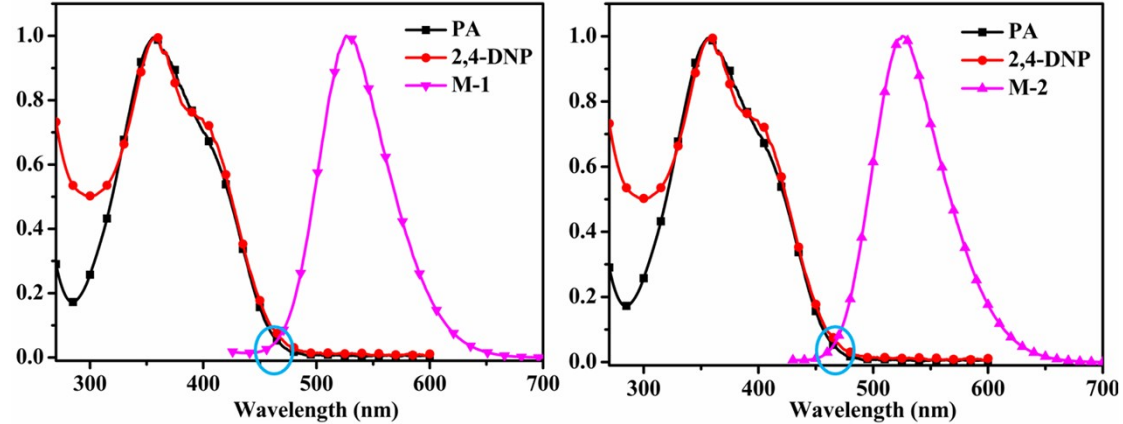


Fig. S10 Normalized absorption spectrum of PA, 2,4-DNP and the fluorescence spectra of **M-1** and **M-2** in THF-water ($f_w = 90\%$) mixture solution.

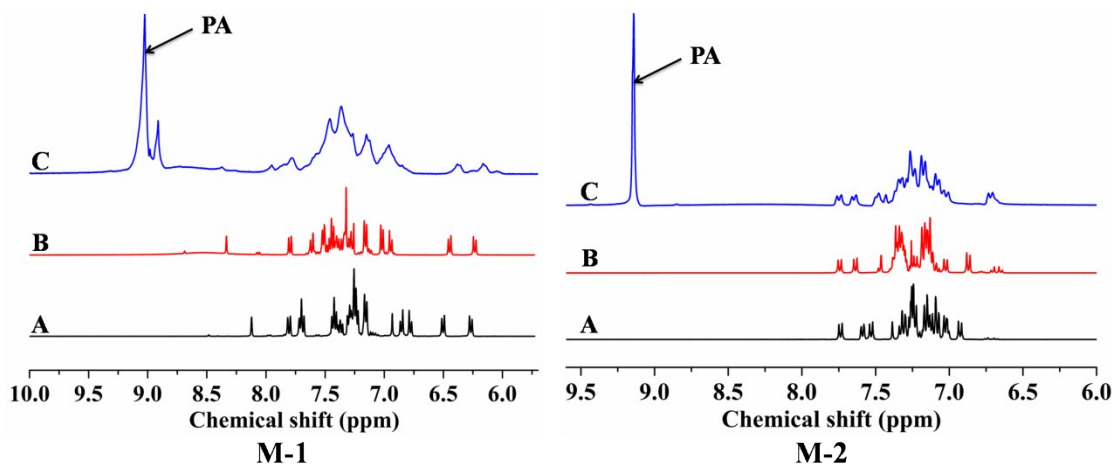


Fig. S11 ^1H NMR spectra of **M-1** and **M-2** in CDCl_3 with **M-1** and **M-2** (A); **M-1** and **M-2** + 2 equivalents TFA (B); **M-1** and **M-2** + 2 equivalents PA (C).

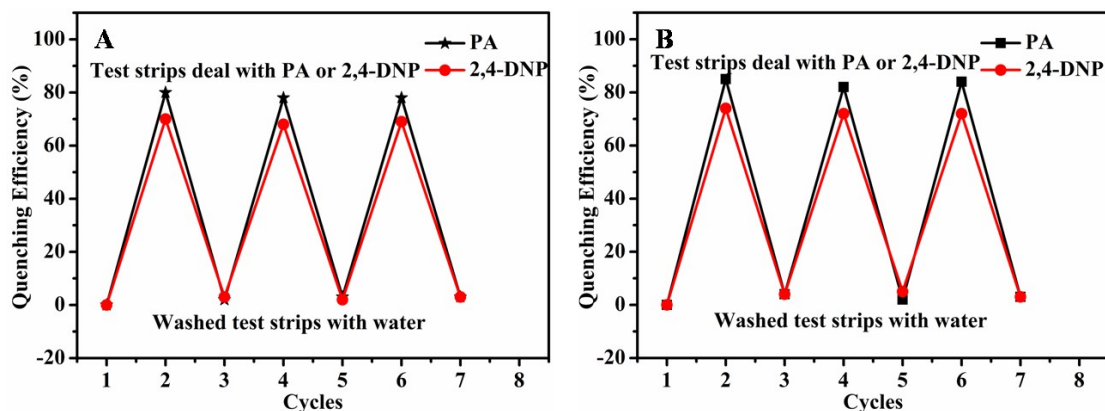


Fig. S12 Reversibility experiment of fluorescent test strips of compound **M-1** (A) and **M-2** (B) for PA and 2,4-DNP detection by washing with water.